Description of proton elastic scattering on ^{6,7,9,11}Li with microscopic effective interaction

Michio Kohno
Physics Division, Kyushu Dental College, Manazuru 2-6-1, Kokurakita-ku, Kitakyushu 803, Japan
(Received 11 May 1993)

Proton elastic scattering on Li isotopes ^{6,7,9,11}Li at $E_p \sim 60$ MeV is described by a nonlocal optical model potential which is constructed by folding a microscopic density-dependent effective interaction with Hartree-Fock single-particle wave functions of the target nuclei. Experimental data are well-described systematically from ^{6}Li to ^{11}Li by our model calculation, implying that the underlying microscopic theory is applicable even at the extreme circumstance of the neutron drip line limit.

PACS number(s): 25.40.Cm, 24.10.Ht, 21.60.Jz, 27.20.+n

Recent measurements [1] of differential cross sections of proton elastic scattering on ^{9}Li and ^{11}Li at $E_p = 60$ and 62 MeV, respectively, have brought us an interesting opportunity to investigate nuclear effective interaction under unusual circumstances. Since the last two neutrons of the ^{11}Li are bound very weakly, the wave function of these neutrons spreads far outside of the residual core part. The breakup cross sections [2] of ^{11}Li on Pb at 800 MeV/c suggests that the rms radius of ^{11}Li is larger than 3 fm. This nonstandard neutron distribution might produce some peculiar effects on the proton scattering on ^{11}Li, which may, in turn, shed some light on the nucleon-nucleus scattering dynamics. A nuclear system is self-governed in the sense that the interactions between nucleons in nuclear medium are highly renormalized by the presence of surrounding nucleons on the one hand, and the nuclear structure arises as a result of these medium-dependent effective interactions on the other. Since we have experimental data for the proton elastic scattering also on ^{6}Li and ^{7}Li at $E_p = 65$ MeV from Research Center for Nuclear Physics (RCNP) [3], we can carry out systematic studies of proton scattering on Li isotopes from $A = 6$ to 11 to test the usual way of understanding nuclear systems.

Studies with a phenomenological potential of the Woods-Saxon type was carried out for ^{9}Li and ^{11}Li in Ref. [2], concluding that an unusual shape of the potential is necessary for ^{11}Li both in real and imaginary parts. There have been several other studies [4] of the proton scattering on ^{11}Li, aiming to examine the role of very weakly bound neutrons. In this report we straightforwardly apply the nuclear matter approach of an optical model potential to the proton scattering on Li isotopes including ^{11}Li to see to what extent the standard microscopic model works.

In the nuclear matter approach of an optical model potential, a scattering matrix is first evaluated in nuclear matter and then is applied to finite nuclei through a local density approximation. The framework has been successful [5–7] to relate the two-body nuclear force with scattering processes of nucleons on nuclei. One difficulty exists, however. The imaginary part of the optical model potential is overestimated, when the scheme is applied to closed-shell nuclei. Namely the strength of the imaginary potential has to be weakened by a factor of 0.7–0.8 to reproduce experimental cross sections. This is connected to the fact that the state density near the Fermi surface in nuclear matter is larger than that in finite closed-shell nuclei. Since the magnitude of the inelasticity is directly governed by the available phase space, the imaginary potential tends to be overestimated. With this problem in mind we will introduce, as usual, an overall renormalization factor in the imaginary part in our calculations.

We construct an optical model potential U by folding complex G matrices with wave functions of a target nucleus:

$$\langle p|U|p\rangle = \sum_h (\langle ph|G_{\rm eff}|ph\rangle - \langle ph|G_{\rm eff}|hp\rangle) + \frac{1}{2}\sum_{h,h'}\left[\left\langle hh'\left|\frac{\delta G_{\rm eff}}{\delta\rho}\right|hh'\right\rangle - \left\langle hh'\left|\frac{\delta G_{\rm eff}}{\delta\rho}\right|h'h\right\rangle\right], \quad (1)$$

where p stands for a scattering nucleon, h and h' for single-particle states of a target nucleus, and ρ denotes the nucleon number density of a target nucleus. Details of explicit calculations of the potential can be found in Ref. [8]. The first two terms are direct and exchange potentials corresponding to the diagrams (a) and (b) of Fig. 1, respectively. Since we take into account exchange terms explicitly, the potential U is nonlocal. The remaining two terms arise naturally when the mean field is defined through variation in the Hartree-Fock approximation for the ground state, which are so-called Pauli rearrangement potentials [9]. However, optical potentials are not defined variationally. Thus, we have to resort to diagrammatical arguments to include these contributions. The inclusion of these terms corresponds to take into account effects which arise basically due to the change of Pauli blocking in the correlation of two nucleons in the target nuclei when an incoming nucleon is added to the target nucleus. These effects are to be depicted as the diagram (c) of Fig. 1.

For the effective G matrices $G_{\rm eff}$ we employ the complex effective interaction called CEG which was parametrized by Yamaguchi, Nagata, and Michiyama [10] based on the G-matrix calculations in nuclear matter using Hamada-Johnston potential [11]. This effective in-

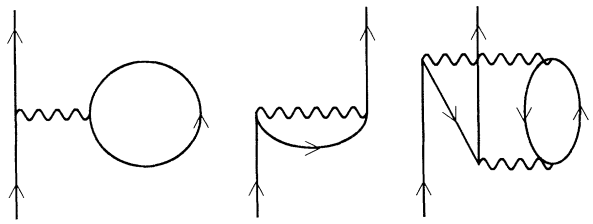

FIG. 1. Diagrams contributing to the optical-model potential.

teraction is energy dependent, designed for the energy range of $65 < E_p < 200$ MeV. In the paper by Yamaguchi, Nagata, and Michiyama the CEG was applied to describe proton scattering on ^{40}Ca, ^{90}Zr, and ^{208}Pb at $E_p = 65$ MeV, and also on ^{12}C, ^{16}O, and ^{208}Pb at higher energies. Experimental data are well reproduced by their calculations. We use the CEG for the proton elastic scattering on Li isotopes at $E_p = 60-65$ MeV. As for the spin-orbit force, we use, instead of the finite-ranged one given in Ref. [10], a δ-type $l \cdot s$ force which has been used for Hartree-Fock calculations [8,12,13]:

$$V_{ls}(\mathbf{r}) = iB(\sigma_1 + \sigma_2)\cdot[\overleftarrow{\nabla}_r \times \delta(\mathbf{r})\vec{\nabla}_r] \quad \text{with } B = 130 \text{ MeV fm}^5 , \tag{2}$$

where r is a relative coordinate.

Since we are interested in global systematics from ^{6}Li to ^{11}Li and not in effects of specific structure of each nucleus, we assume spherical single-particle orbits and average occupation. We prepare single-particle wave functions of target nuclei by density-dependent Hartree-Fock calculations reported in Ref. [13]. Hartree-Fock calculations have the advantage of being able to follow the bulk structural change of nuclei towards the neutron drip-line limit. Although Li isotopes were not explicitly discussed in Ref. [13], binding energies are rather well-reproduced as shown in Table I. Of course we do not expect a perfect agreement of Hartree-Fock calculations with experiments. Hence we introduce some modifications of effective interactions for ^{7}Li and ^{11}Li to try to obtain closer agreement with experiments, though the prescription cannot be unique. For ^{11}Li it is essential to reproduce very shallow binding of the $0p_{1/2}$ neutron, which leads to a large rms radius. To achieve it, the strength of the ^{3}E force is reduced by about 25% when the $0p_{1/2}$ neutron is concerned. For ^{7}Li shallower single-particle energies by 7 MeV are inserted in the energy-dependent terms of the effective force to make the overall interaction a little more attractive. Original results are shown in parentheses in Table I. In ^{11}Li the rms radius is seen to be improved from 2.82 fm to 3.24 fm. Later we will observe the consequence of this difference of single-particle wave functions of ^{11}Li in calculated differential cross sections.

It is worthwhile to comment about quadrupole moments of ^{9}Li and ^{11}Li. In these two nuclei, neutrons are supposed to fill the single-particle orbits up to $0p_{3/2}$ and $0p_{1/2}$, respectively. Thus the quadrupole moment is to be generated by a single proton in the $0p_{3/2}$ orbit. In this picture the quadrupole moment has a plain relation to the mean square radius of the proton single-particle wave function [16]:

$$Q = -\frac{2j-1}{2j+1}\langle j|r^2|j\rangle , \tag{3}$$

where j denotes a total angular momentum of the proton orbit. Experimental data by Arnold *et al.* [14,15] suggested that the mean radius of the proton in $0p_{3/2}$ orbit is slightly larger in ^{11}Li than in ^{9}Li. Table I shows that our Hartree-Fock calculations reproduce this variation and even the absolute values. The change of the mean square radius implies that rearrangement effects in the ^{9}Li core are not negligible when two neutrons are added.

Calculated cross sections are shown in Figs. 2 and 3, and compared with experimental data. The overall agreement with experiment is good and the characteristics are well-reproduced. That is, the cross sections in ^{7}Li show larger bending at around $\theta_{\text{c.m.}} = 50°$ than in ^{6}Li. In ^{9}Li the cross sections at angles larger than 50° are larger than those in ^{6,7}Li. The diffraction minimum occurs at smaller angle in ^{11}Li.

The parameter N_I which adjusts the strength of the imaginary part of the optical model potential is given in the figure for each scattering. To see how the results are sensitive to this renormalization we show, in Fig. 4, cross sections of proton scattering on ^{11}Li with $N_I = 1.0$, 0.9, and 0.8. We observe that the change of the imaginary strength scarcely affects the overall shape. The magnitude of the renormalization required for each target tells the characteristic of the target. In previous applications [7,10] of the CEG potential for proton scattering on closed nuclei, ^{40}Ca and ^{12}C, N_I was found to be 0.7–0.8.

TABLE I. Density-dependent Hartree-Fock calculations for Li isotopes, using the scheme of Ref. [13]. Effective forces are modified for ^{7}Li and ^{11}Li, separately, to obtain better agreement with experimental energies. The original results are shown in the parentheses. The calculated rms radius includes cm and nucleon finite-size corrections.

	Binding energy (MeV)		rms radius (fm)		Quadrupole moment (fm^2)	
	Expt.	Cal.	Expt. [2]	Cal.	Expt. [14,15]	Cal.
^{6}Li	31.99	32.21	2.54	2.27		
^{7}Li	39.24	39.10	2.50	2.34		
		(36.26)		(2.37)		
^{9}Li	45.34	45.56	2.43	2.54	-27.4 ± 1.0	-27.3
^{11}Li	45.50	45.18	3.27	3.24	-31.2 ± 4.5	-29.3
		(49.39)		(2.82)		(-28.8)

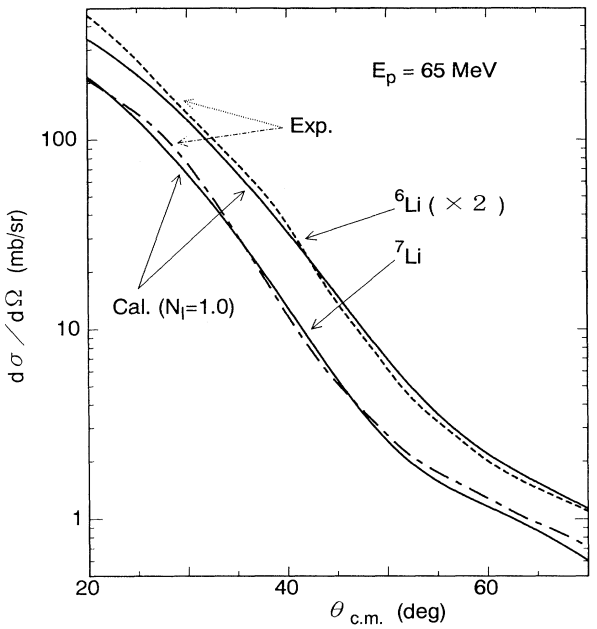

FIG. 2. Angular distributions for proton elastic scattering on ^{6}Li and ^{7}Li at $E_p=65$ MeV. Experimental data shown by the dashed (^{6}Li) and dot-dashed (^{7}Li) curves are taken from Ref. [3]. Calculated results are shown by the solid curves.

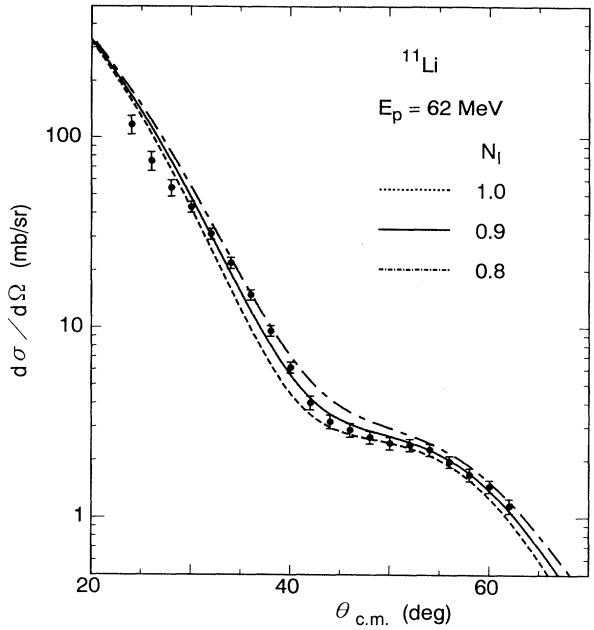

FIG. 4. The dependence of calculated differential cross sections of p-^{11}Li elastic scattering at $E_p=62$ MeV on the renormalization factor N_I.

In our calculation ^{9}Li needs a similar number. Actually neutrons are rather tightly bound in ^{9}Li. On the contrary neutrons in the open shell $p_{3/2}$ of ^{6,7}Li are loosely bound and should have larger phase space for inelastic channels, which leads to a larger imaginary strength of the optical model potential. The large N_I in ^{11}Li agrees. Though neutrons are in closed shells, two neutrons are very loosely bound and hence easily excited. Our result for the renormalization factor necessary to reproduce cross sections is very reasonable and seems to reflect characteristics of the nuclear structure of Li isotopes.

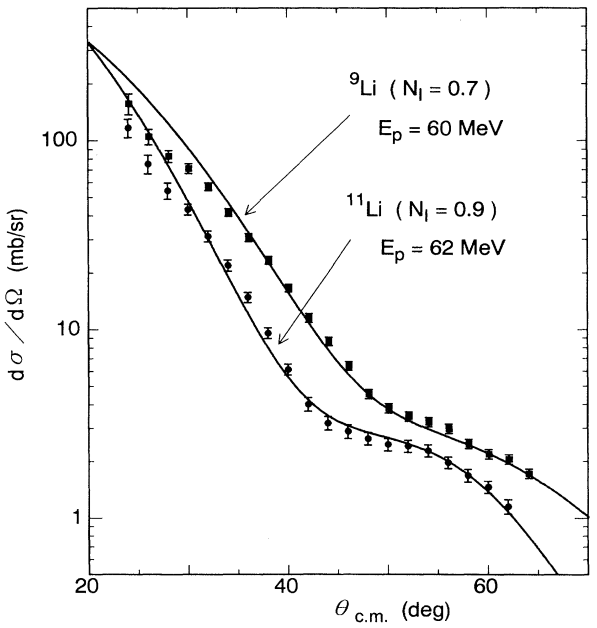

FIG. 3. Angular distributions for proton elastic scattering on ^{9}Li and ^{11}Li at $E_p=60$ and 62 MeV, respectively. Experimental data are from Ref. [1]. The renormalization factor N_I for the imaginary potential is 0.7 for ^{9}Li and 0.9 for ^{11}Li.

In order to see the role of the density-dependence of the effective interaction, we repeat calculations for ^{11}Li by fixing the density to be used in the interaction at $\rho=\rho_0$, $\rho_0/2$,$\rho_0/4$, and $\rho_0/8$ with $\rho_0=0.17$ fm^{-3} being normal nuclear density. Results shown in Fig. 5 clearly indicate the significant effects of the density dependence of the interaction. Similar results are seen also for ^{6}Li, ^{7}Li, and ^{9}Li.

Next we show the consequence of the improvement of single-particle wave functions of ^{11}Li. As noted before we modified the effective force for the Hartree-Fock calculation of ^{11}Li, which improved the rms radius from 2.82 fm to 3.24 fm. The differential cross sections evaluated with these two sets of ^{11}Li wave functions are shown in Fig. 6. It is interesting to see that the improved wave functions give a better agreement with experiments.

We have calculated differential cross sections of proton elastic scatterings on Li isotopes, using the microscopic framework of an optical model potential. The experimental data of proton elastic scattering on ^{6,7,9,11}Li provide an interesting possibility to compare scattering processes in various conditions of the target nuclear structure. The microscopic model is supposed to follow the change of the target nuclei, structural and isotopical. Our calculations have demonstrated that the microscopic model of an optical model potential can provide an overall good description of the proton elastic scattering cross section on Li isotopes from ^{6}Li to ^{11}Li. It indicates that the underlying microscopic theory of nuclear matter

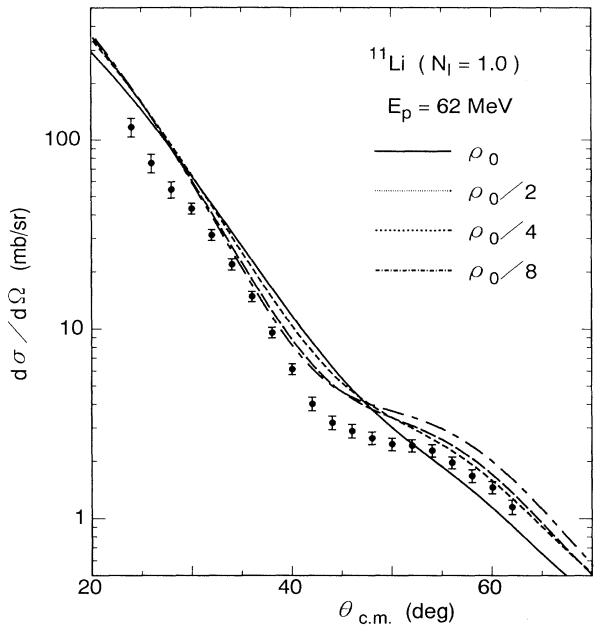

FIG. 5. Angular distributions for p-^{11}Li elastic scattering at $E_p = 62$ MeV, obtained with the prescription in which the density to be used in the effective interaction is taken to be constant: $\rho = \rho_0$, $\rho_0/2$, $\rho_0/4$, and $\rho_0/8$ with $\rho_0 = 0.17$ fm^{-3} being normal nuclear density.

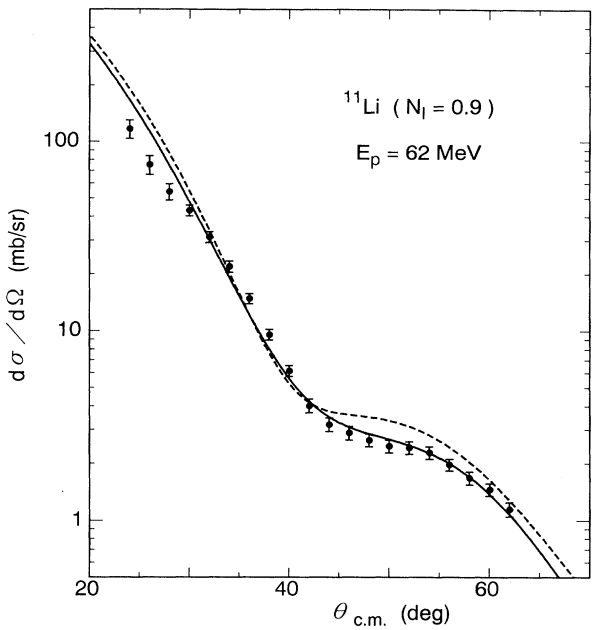

FIG. 6. Differential cross sections calculated with different wave functions of ^{11}Li. The solid curve is the same as in Fig. 3. The dotted curve is obtained using wave functions which have a smaller rms radius.

approach for an optical model potential, as well as the description of these target nuclei, is reasonble.

There are some problems to be studied in the future. There should be some specific features in each of the Li isotopes. The spherical mean-field description of Li isotopes used in our calculation is only the starting approximation. We may also be interested in dynamical effects such as break-up effects and long-range pairing, which reflect the structure of target nuclei. The scattering-effective interaction is also to be revised. First, certain modifications may be needed, corresponding to the modifications of the effective interactions for ground-state wave functions of ^{11}Li and ^{7}Li. Second, since the CEG [10] was parametrized based on the G matrices in symmetric nuclear matter, some corrections are expected when we consider the application to asymmetric nuclear systems. These problems may be related to the discrepancy between experimental and calculated cross sections at forward angles.

The author is grateful to D.W.L. Sprung for helpful suggestions.

[1] C. B. Moon, M. Fujimaki, S. Hirenzaki, N. Inabe, K. Katori, J. C. Kim, Y. K. Kim, T. Kobayashi, T. Kubo, H. Kumagai, S. Shimoura, T. Suzuki, and I. Tanihata, Phys. Lett. B **297**, 39 (1992).

[2] I. Tanihata, H. Hamagaki, O. Hashimoto, S. Nagamiya, Y. Shida, N. Yoshikawa, O. Yamakawa, K. Sugimoto, T. Kobayashi, D. E. Greiner, N. Takahashi, and Y. Nojiri, Phys. Lett. **160B**, 380 (1985); I. Tanihata, H. Hamagaki, O. Hashimoto, Y. Shida, N. Yoshikawa, K. Sugimoto, O. Yamakawa, T. Kobayashi, and N. Takahashi, Phys. Rev. Lett. **55**, 2676 (1985); I Tanihata, T. Kobayashi, O. Yamakawa, S. Shimoura, K. Ekuni, K. Sugimoto, N. Takahashi, T. Shimoda, and H. Sato, Phys. Lett. B **206**, 592 (1988).

[3] M. Tosaki, Ph.D. thesis, Osaka University, 1989.

[4] Y. Suzuki, K. Yabana, and Y. Ogawa, Phys. Rev. C **47**, 1317 (1993).

[5] J. P. Jeukenne, A. Lejeune, and C. Mahaux, Phys. Rep. **25C**, 83 (1976).

[6] F. Brieva and J. R. Rook, Nucl. Phys. **A291**, 299 (1977); **A291**, 317 (1977).

[7] N. Yamaguchi, S. Nagata, and T. Matsuda, Prog. Theor. Phys. **70**, 459 (1983).

[8] X. Campi and D. W. L. Sprung, Nucl. Phys. **A194**, 401 (1972).

[9] J. W. Negele, Phys. Rev. C **1**, 1260 (1971).

[10] N. Yamaguchi, S. Nagata, and J. Michiyama, Prog. Theor. Phys. **76**, 1289 (1986).

[11] T. Hamada and I. D. Johnston, Nucl. Phys. **34**, 382 (1962).

[12] M. Beiner, H. Flocard, Nguyen Van Giai, and P. Quentin, Nucl. Phys. **A238**, 29 (1975).

[13] M. Kohno, S. Nagata, and N. Yamaguchi, Prog. Theor. Phys. Suppl. **65**, 200 (1979).

[14] E. Arnold *et al.*, Z. Phys. A **331**, 295 (1988).

[15] E. Arnold *et al.*, Phys. Lett. B **281**, 16 (1992).

[16] A. Bohr and B. Mottelson, *Nuclear Structure* (Benjamin, New York, 1975), Vol. I.